Linear Dichroism of Solute Molecules within Micelles. 2.[1] Preferred Orientations and Local Ordering

Michel Laurent*[†] and Bruno Samorì*[‡]

Contribution from ENS, Laboratoire de Physique, 92211 Saint-Cloud, France, and Dipartimento di Chimica Organica, Università degli Studi, Viale Risorgimento 4, 40136 Bologna, Italy.
Received November 6, 1986

Abstract: A linear dichroism (LD) approach for determining solute orientations within anionic micelles, and for making use of the intrinsic anisotropies of chemical and photochemical processes inside micellar systems, was recently reported (part 1). In this paper we use this technique to attain also a *quantitative picture of the local ordering* achieved by a guest molecule within its host micelle. This picture of the anisotropy of the solute orientational distribution within its solubilization site may be particularly useful in the micellar catalysis and membrane mimetic chemistry. This paper also extends the LD technique to all types of lyotropic nematic solvents (N_{C^+}, N_{D^+}, N_{C^-}, N_{D^-}). Orange Red is our guest molecular probe. The local orientation of its molecular long axis proved to be preferentially perpendicular to the host micelle surface. The local ordering of the same guest molecule was found to be surprisingly high if one takes into account the emphasis so far put by many authors on the inner disorder of the micellar aggregates. We have also found that the N_{D^+} micelles provide the highest linear anisotropy achievable in oriented samples by micellar systems. This result shows the way to make the most effective use of the intrinsic anisotropy of photochemical processes, also within the micellar chemistry field.

A new linear dichroism (LD) approach for determining solute orientations within anionic micelles was recently published.[1] This approach provides a way to attain easy-to-control orientational effects and may even suggest means of revealing and making use of the intrinsic anisotropies of chemical and photochemical processes inside micellar systems.[2-4]

This new approach is based on the joint use of the LD technique[5,6] and lyotropic nematic liquid crystals. The first LD approach to solute orientation in a lyotropic nematic system was reported by Johansson et al.[7a] Measurements were recently carried out also by Labes et al.[7b,c] The building units of lyotropic nematic liquid crystals are weakly anisometric rod- or disk-like micelles.[8] Nematic disk-like, N_D, phases occur as the precursors to the lamellar phase, while the cylindrical N_C's are the precursors to the hexagonal phase. Information about guest orientation within nematic micelles can be transferred and utilized in chemically corresponding classical micellar solutions, where orientational studies cannot be carried out because of their isotropy.[1]

The model of solubilization presented in ref 1 provides a general framework for analyzing LD spectra in rod-like micelles and also allows orientational data to be interpreted on a stereochemical basis. In addition, the usefulness of the technique in revealing specific guest-host interactions is displayed there by employing weakly anisometric aromatic molecules as absorbing solutes. Their overall macroscopic ordering was very small and their order parameters span a very small area within their possible field of variation (see, in particular, Figure 5 of ref 1). The LD measurements of these small-order parameters were made possible by the very sensitive modulated technique.[6]

The present paper intends to span the regions of the highest order parameters achievable, by using now a static set-up of the LD measurements which is more convenient than the modulated one for this purpose. This paper also intends to allow the technique to attain a quantitative picture of the local order achieved by the guest molecule within its host micelle. The technique is extended to all types of lyotropic nematic solvents (N_{C^+}, N_{D^+}, N_{C^-}, N_{D^-}),[10-13] checking also possible dependencies of the guests ordering upon the micelle shape.

Orange Red was chosen as orientation probe because of its very anisotropic shape and high-order parameters in thermotropic mesophases,[14] because of its possible ability to grasp at the host polar head surfaces (as discovered in nitrogenated hydrocarbons[1]), and also because of its length which is comparable to that of the soaps of the host aggregate. In all the different types of micelles

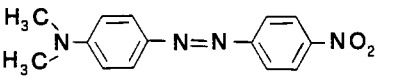

used throughout this investigation, the *local orientations of the long-axis of Orange Red proved to be preferentially perpendicular to the micelle surface as well as very high and poorly dependent on micelle shape.*

Experimental Section

The lyotropic mixtures were prepared according to the procedure described in ref 1. The compositions (in percentage by weight) and the aggregate types are reported in Table I. The guest Orange Red concentration was about 3×10^{-4} M which always corresponds to less than one molecule per host aggregate. We verified, by microscopic observations, that the dye dissolution does not affect the sample texture.

[†]ENS, Laboratoire de Physique.
[‡]Dipartimento di Chimica Organica (Bologna).

(1) Part 1: Samorì, B.; Mattivi, F. *J. Am. Chem. Soc.* **1986**, *108*, 1679-1684.
(2) Menger, F. M. *Surfactants in Solution*; Mittal, K. L., Lindman, B., Eds.; Plenum: New York, 1984; Vol. 1, pp 347-357. Menger, F. M.; Doll, D. W. *J. Am. Chem. Soc.* **1984**, *106*, 1109-1113.
(3) (a) Bunton, C. A. *Solution Chemistry Surfactants* (Proc. Sect. 52nd Colloid Surf. Sci. Symp.); Mittal, K. L., Ed.; Plenum: New York, 1979; Vol. 2, pp 519-540. (b) Tonellato, U. *Ibid.* pp 541-558. (c) Fendler, J. H.; Fendler, E. J. *Catalysis in Micellar and Macromolecular Systems*; Academic Press: New York, 1975.
(4) Turro, N. J.; Grätzel, M.; Braun, A. M. *Angew. Chem., Int. Ed. Engl.* **1980**, *19*, 675-696. Fendler, J. H. *Chem. Eng. News* **1984**, *62*(1), 25-38, Love, L. J. C.; Habarta. J. G.; Dorsey, J. G. *Anal. Chem.* **1984**, *56*, 1132A-1148A.
(5) Michl, J.; Thulstrup, E. W. *Polarized Spectroscopy: Partially Aligned Solutes*; Verlag-Chemie: Weinheim, 1986. Thulstrup, E. W.; Michl, J. *J. Am. Chem. Soc.* **1982**, *104*, 5594-5604.
(6) Samorì, B. *Mol. Cryst. Liq. Cryst.* **1983**, *98*, 385-397. Samorì, B.; Mariani, P.; Spada, G. P. *J. Chem. Soc., Perkin Trans. 2* **1982**, 447-453.
(7) (a) Johansson, L. B. A.; Söderman, O.; Fontell, K.; Lindblom, G. *J. Phys. Chem.* **1981**, *85*, 3694-3697. (b) Kuzma, M. R.; Skarda, V.; Labes, M. M. *J. Chem. Phys.* **1984**, *87*, 2925-2957. (c) Skarda, V.; Labes, M. M. *Mol. Cryst. Liq. Cryst.* **1985**, *126*, 187-195.
(8) (a) Hendrix, Y.; Charvolin, J.; Rawiso, M.; Liebert, L.; Holmes, M. C. *J. Phys. Chem.* **1983**, *87*, 3991-3999. (b) Charvolin, J.; Hendrikx, Y. *Nuclear Magnetic Resonance of Liquid Crystals*; Emsley, J. W., Ed.; Reidel: Dordrecht, Holland, 1985; pp 449-471. (c) Hoffman, H. *Ber. Bunsenges. Phys. Chem.* **1984**, *88*, 1078-1093.
(9) (a) Fujiwara, F. Y.; Reeves, L. W. *J. Phys. Chem.* **1980**, *84*, 653-661. (b) Radley, K.; Reeves, L. W. *Can. J. Chem.* **1975**, *53*, 2998.
(10) Yu, L. J.; Saupe, A. *Phys. Rev. Lett.* **1980**, *45*, 1000.
(11) Long, R. C.; Goldstein, J. H. *Liquid Crystals and Ordered Fluids*; Johnson, J. F., Porter, R. S., Eds.; Plenum Press: New York, 1974; Vol. 2, pp 147-160.
(12) Forrest, B. J.; Reeves, L. W.; Robinson, C. J. *J. Phys. Chem.* **1981**, *85*, 3244.
(13) Holmes, M. C.; Boden, N.; Radley, K. *Mol. Cryst. Liq. Cryst.* **1983**, *100*, 93-102.
(14) Jones, F.; Reeve, T. J. *Mol. Cryst. Liq. Cryst.* **1980**, *60*, 99-110.

0002-7863/87/1509-5109$01.50/0

Table I[a]

mixture	N_{C^+}		N_{C^-}		N_{D^+}		N_{D^-}	
(1)	D_2O	64.8	(4) D_2O	55.9	(5) D_2O	48.9	(7) D_2O	60.0
	KL	33.0	KHxOB	36.5	KHxOB	39.1	KL	30.0
	KCl	2.2	dOH	7.6	dOH	5.8	dOH	6.0
					Na_2SO_4	6.2	KCl	4.0
(2)	D_2O	56.9			(6) D_2O	62.6	(2)	as in N_{C^+}
(t > 28 °C)	SdS	35.9			KL	17.5		(t < 28 °C)
	dOH	7.2			KHpOB	12.4		
(3)	D_2O	67.8			dOH	5.3	(3)	as in N_{C^+}
(t > 25 °C)	KL	26.0			KCl	2.2		(t < 25 °C)
	dOH	6.2						

[a] KL = potassium laurate; KHxOB = potassium hexyloxybenzoate; KHpOB = potassium heptyloxybenzoate; SdS = sodium decylsulfate; dOH = decanol.

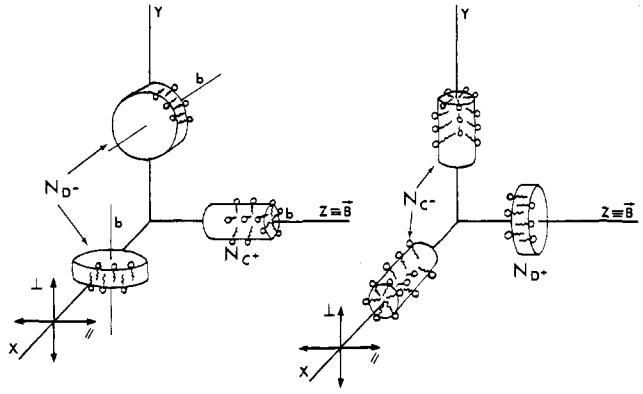

Figure 1. Preferred orientations of the four classes of lyotropic nematic micelles. The cylindrically shaped ones (N_C), depending on the diamagnetic anisotropy of the soap hydrocarbon chains, may tend to stay parallel (N_{C^+}) or perpendicular (N_{C^-}) to the orienting magnetic field (B). Also disk-like micelles which preferentially align their C_∞ axes to B (N_{D^+}) or to planes perpendicular to B (N_{D^-}) may be prepared. The incoming light is propagating in our samples along X, and its directions of polarization, parallel (∥) and perpendicular (⊥) to the Z direction are also depicted.

The LD measurements were made with the static method. Sample orientations were obtained by a 1.2-T magnetic field which was inserted directly into the beam path. The temperature was controlled to ±0.05 °C.

Results and Discussion

A sample is said to exhibit LD when light absorption depends on the direction of the linear polarization of the beam. LD is usually defined as the differential absorption $[E_\parallel - E_\perp]$ of two plane-polarization components of an electromagnetic radiation, where the parallel (∥) and perpendicular (⊥) directions refer to the optical axis, or director, of the oriented sample.

The LD signals were obtained by the static technique[5] which provides the single $E_\parallel$ and $E_\perp$ spectra. The reduced LD for the static measurements is

$$LD_r = 3(E_\parallel - E_\perp)/(E_\parallel + 2E_\perp) \quad (1)$$

For an isolated transition polarized along the j direction

$$LD_r = 3S_{jj} \quad (2)$$

$$S_{jj} = \tfrac{1}{2}\langle 3\cos^2\theta_{j,Z} - 1\rangle \quad (3)$$

where the order parameter S_{jj} is a diagonal tensor[15] averaged over all the guest molecules. $\theta_{j,Z}$ are the deflection angles from the sample director Z of the j direction within the guest molecular framework.

All four classes of anisometric micelles[8-13] were spanned by this study. Soaps with aliphatic hydrocarbon chains tend to stay perpendicular to the magnetic field B, thus leading to aggregates with their C_∞ axes preferentially parallel or perpendicular to B for cylinders (N_{C^+}) and disks (N_{D^+}), respectively (Figure 1). Soaps with fluorocarbon chains or phenyl rings, having opposite diamagnetic anisotropy, lead to aggregates with the tendency to orient their C_∞ axes perpendicular to B for cylinders (N_{C^-}) or parallel to B for disks (N_{D^+}) (Figure 1).[11,12]

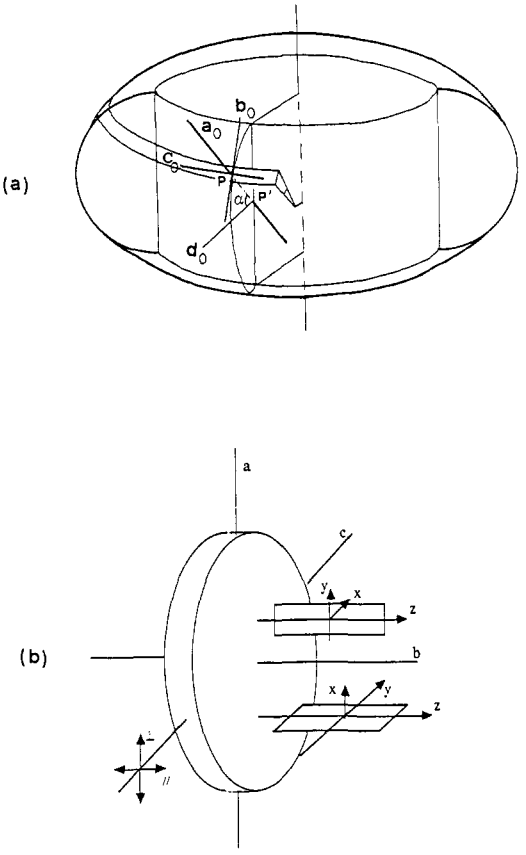

Figure 2. (a) A central disk, flat and bilayered, which is rounded off by a rim, constitutes our model of N_D micelles. The a_0 axis is connecting P to the half-height P' point of the lateral surface of the disk bilayer. The angle α is therefore defined at that point P' by a_0 and a d_0 axis perpendicular to the micelle axis b. (b) Limiting solubilization modes for a lath-like guest molecule which tends to intercalate perpendicular to the disk surface of the host disk-like micellar aggregate. The two limiting orientations which together represent the free rotation of the guest molecules around their z axes are depicted here. The directions of propagation (c) and polarizations ∥ and ⊥ of the incoming beam are shown as for a N_{D^+} micelle.

The prolate spheroidal shape of the N_C micelles can be depicted by a cylindrical model completed by a couple of terminal hemispherical caps. Being on the whole geometrically isotropic, these caps merely decrease the overall linear anisotropy of the cylindrical surface offered to guest molecule implantations.[1] A flat, bilayered disk, which is rounded off by a rim, may instead be used for the N_D oblate spheroids (Figure 2a). These micelles were also labeled type I or type II depending on whether their C_∞ axes tend to align parallel or perpendicular to the field.[16]

(15) Zannoni, C. *Nuclear Magnetic Resonance of Liquid Crystals*; Emsley, J. W., Ed.; Reidel: Dordrecht, Holland, 1985; pp 1-31.

(16) Forrest, B. J.; Reeves, L. W. *Chem. Rev.* **1981**, *81*, 1-14.

Table II

	phase (mixture no.)								
	N_{C^+}			N_{C^-}	N_{D^+}		N_{D^-}		
	(1)	(2)[a]	(3)[b]	(4)	(5)	(6)	(7)	(2)[c]	(3)[d]
LD_r	−0.275	−0.377	−0.285	0.281	0.75	0.527	−0.353	−0.383	−0.297
$S_{zz}^{exp.}$	−0.092	0.125	−0.095	0.094	0.25	0.176	−0.118	−0.128	−0.099
$(S_{zz})_{max}$		−0.5		0.25		+1.0		−0.5	
exptl r/L or h/R		0.38[e]	0.67[e]					1.08[e]	1.12[e]
$(S_{zz}^{exp})_{cor}$	−0.214[f]	−0.22	−0.222	0.219[f]	0.5[f]	0.32[f]	−0.275[f]	−0.29	−0.233
$(S_{zz})_{max}/(S_{zz}^{exp})_{cor}$	0.43	0.44	0.44	0.88	0.50	0.32	0.55	0.58	0.47

[a] $t > 28$ °C. [b] $t > 25$ °C. [c] $t < 28$ °C. [d] $t < 25$ °C. [e] Reference 8a. [f] Corrected-order parameters obtained by using the r/L and h/R values experimentally estimated for the N_{C^+} and N_{D^-} phases of (3).[8a]

It is also possible to induce transitions between N_C and N_D phases, just by changing the temperature of specific mixtures. We can therefore *follow in the same sample the orientation of a guest molecule while the micelle shape is changing.* We did it by dissolving Orange Red in mixtures 2 and 3 which are N_{D^-} below 28 and 25 °C, respectively, and N_{C^+} >28 and 25 °C (see Table I).[9b,10]

Experimental-Order Parameters: S_{zz}^{exp}

Table II reports the LD_r values exhibited by the dye's visible band at various temperatures, in the different mesomorphic solvents. The long-axis (z) polarization of the electronic transition responsible for the recorded absorption signal can be inferred from the results of ref 14. The S_{zz}^{exp} values thus obtained by eq 2 clearly display the *tendency of the guest dye to follow a B-like intercalation mode,*[1] *i.e., to align its long axis with the extended soap chains of the host aggregate.*

Limiting-Orientation Modes and Limiting-Order Parameters: $(S_{zz})_{max}$

It must be always taken into account that the experimental-order parameters must be used very cautiously for stereochemical purposes. By themselves, they provide a very incomplete specification of orientational distributions particularly in the cases, like this one, where the guest molecule may find different sites available for its location within the host. Keeping this well in mind, models of orientational distributions can be suggested on the basis of the guest–host symmetries and stereochemistries. Along these lines a very simple geometrical method capable of giving signs and limiting values of the order parameters for all the limiting guest orientations compatible with the guest–host stereochemistry was previously developed for N_{C^+} micelles only.[1] In this paper, this approach is extended to the solubilization of Orange Red in N_{C^-}, N_{D^+}, and N_{D^-} host micelles.

The tendency of this guest molecule to align its long axis with the extended soap chains of the host aggregate, reflected in its S_{zz}^{exp} values, limits the problem to solubilization modes which were labeled as type B in the N_{C^+} case.[1]

The maximum values corresponding to the limiting orientation mode B within the anisometric parts of the different micelles are reported in Table II as $(S_{zz})_{max}$.

Cylindrical Micelles. On passing from N_{C^+} to N_{C^-}, the value of −0.5[1] changes sign and becomes 0.25; this is because the micelle's long axis moves from a preferred Z axis alignment to a random distribution in the laboratory XY plane. The two limiting orientations along the X and Y axes, shown in Figure 1, represent this new orientational distribution, and only that with the micelle long axis b directed along Y contributes to the LD. It must also be pointed out that wall effects may tend to favor the Y alignment with respect to the X alignment. The relevance of this effect is expected to increase when the cell path is reduced, and may therefore lead to experimental-order parameters even higher than the theoretical $(S_{zz})_{max} = 0.25$ which is expected for an equal population of the X and Y alignment.

Disk-like Micelles. Figure 2b shows the two limiting solubilization modes for a lath-like guest molecule which tends to intercalate perpendicularly to the disk surface of the host N_{D^+} micellar aggregate. The two limiting orientations are not discriminated by the micellar structure and together represent the free rotation of the guest molecules around their z axes.

Table III

guest distribution	limiting orientations	S_{xx}	S_{yy}	S_{zz}
(B) intercalation of a lath-like guest with the molecular long z axis aligned with the extended soap chains	(bz, cx)	−	$-1/2$	$+1/2$
	(bz, cy)	$-1/2$	−	$+1/2$
	$(S_{uu})_{max}$	$-1/2$	$-1/2$	+1

Table III gives the contributions to $(S_{uu})_{max}$ of these two preferred limiting orientations, labeled (bz, cx) and (bz, cy). In these two limiting modes the micelle b and c axes are perfectly aligned to the z and x or to the z and y molecular axes, respectively. The maximum molecular alignment, with respect to the magnetic field, is therefore twice that which can be achieved by the corresponding N_C systems.

In moving from N_{D^+} to N_{D^-} the values of $(S_{zz})_{max}$ reverses its sign and becomes $1/2$ because, as with N_{C^-}, no contributions are given to the LD by the limiting arrangement (Figure 1) where the micelle b axis is aligned to the propagation of the incoming polarized beam, since the z-polarized transition moments are now preferentially aligned to the micelle b axis (Figure 2b) and cannot absorb.

It must be pointed out that $(S_{zz})_{max}$ equals unity only in the N_{D^+} case. These micelles provide the most efficient lyotropic matrix to get the highest macroscopic anisotropy achievable. This theoretical prediction is very important for photochemical applications of micellar hosts. The experimental LD values obtained by us with the N_{D^+} micelles are indeed much higher than all others confirming this prediction.

Comparison of $(S_{zz})_{max}$ and S_{zz}^{exp} Values

The $(S_{zz})_{max}$ values are in all cases much larger than the corresponding experimental values S_{zz}^{exp}. The $(S_{zz})_{max}$ values were obtained by considering the micelles as infinite rods or disks, i.e., far more anisometric than they really are in both N_C and N_D mesophases. An alternative view is that the guest molecules were assumed to be dissolved only within the parts of the micelle structures which mostly determine the linear anisotropy of the sample: the cylindrical and the disk-like central parts of the two models. In fact, the two hemispherical caps or the rim, which along with the two above parts constitute the two models, also offer surfaces for guest implantations and decrease the overall linear anisotropy of the system. Since the S_{zz}^{exp} *values describe the macroscopic linear anisotropy of the sample, they underestimate the local ordering of the guest molecules within the host aggregates because they include contributions from the molecules dissolved within the caps or the rims of the host micelles.*

If we want to make use of such orientational information in the micellar catalysis field and in membrane mimetic chemistry, we must "translate" it in terms of *local anisotropy* of the solute orientational distributions within its solubilization site.

Macroscopic Ordering and Local Ordering

The highly elegant and effective approach put forth by Norden to describe the orientation of solute molecules in stretched polymer matrices[17] may be transferred to this problem. It will enable us

to relate the S_{jj} order parameter to the structural constitution of our system. It can be actually split into two uncorrelated and uniaxial orientation systems: that of the b axis of the cylindrical or discoid micelle with respect to the laboratory X, Y, Z frame (Figure 1) and that of the $i = x, y, z$ axes of the guest molecule with respect to the b micelle axis. Their orientation can be described by the order parameters S_a and S'_{ii}, respectively.

The orientational axes i were chosen to provide the orientation of the molecule with respect to the micelle b axis through a diagonal tensor S'_{ii}. When the molecule does not belong a high symmetry group (e.g., C_{2v}), the j directions of the transition moments may lie at a nonvanishing angle $\vartheta_{j,i}$ to the i orientational axes, and must therefore be related to the i axes by the optical factors $O_i = \cos^2 \vartheta_{j,i}$. Thus the S_{jj} tensor and LD_r become

$$S_{jj} = S_a(S'_{xx}O_x + S'_{yy}O_y + S'_{zz}O_z) \quad (4)$$

$$LD_r = 3S_a\sum_i S'_{ii}O_i \text{ for } i = x, y, z \quad (5)$$

These general formulas may also be used to describe the single limiting solubilization models A–D of the previous paper.[1] The S'_{ii} symbols then take the values of the maximum order parameters computed for these A–D guest distributions (Table I of ref 1). If we let the molecule belong also to low symmetry groups, the O_i values are for in-plane polarized transitions: ($O_z = \cos^2 \vartheta_{j,z}$; $O_y = \sin^2 \vartheta_{j,z}$; $O_x = O$), and we obtain therefore for the A–D solubilization modes

$$(LD_r)_A = -\tfrac{3}{4}S_a(2 - 3\cos^2 \vartheta_{j,z}) \quad (6a)$$

$$(LD_r)_B = -\tfrac{3}{4}S_a(3\cos^2 \vartheta_{j,z} - 1) \quad (6b)$$

$$(LD_r)_C = -\tfrac{3}{8}S_a \quad (6c)$$

$$(LD_r)_D = \tfrac{3}{4}S_a \quad (6d)$$

In (6c) and (6d) the LD dependence upon $\vartheta_{j,z}$ disappears, as expected, because of the free molecular rotation around the x axis which is allowed by the radial disk-like intercalation (C) and the tangential adsorption (D) modes.

Equations 6a–d may easily give also the S_{ii} limiting values for the A–D limiting orientational modes of Table I in ref 1 and therefore also the $(S_{zz})_{max}$ for the N_{C^+} case in Table I of this paper.

The general formulas 4 and 5 fit both the cylindrical and disk-like case. Correction factors, C and C', will be inserted therein in order to take into account the role of the caps and the rims within the two cases.

Shape-Correction Factor for Cylindrical Micelles. The distribution of the guest molecules is considered to be homogeneous within the surfaces of the cylindrical part ($2\pi rL$) and of the two caps ($4\pi r^2$); each absorption $E_\parallel$ or $E_\perp$ is considered to be constituted by two terms, relative to the two contributions and weighted by the two coefficients $2\pi rL$ and $4\pi r^2$. Then we obtain

$$(LD_r)^{cor} = 3S_a\sum_i S'_{ii}O_i/C \quad (5')$$

$$C = (1 + 2r/L)$$

where r and L in this shape-correction factor are the radius and the length of the cylindrical part of the host aggregate. The dimensions of N_{C^+} and N_{D^-} micelles reported in Table II were estimated by neutron and X-ray diffraction studies.[8a] They have been basically confirmed by very recent freeze–fracture–electron-microscopy measurements.[18]

Furthermore, in case the guest implanation (like micelle composition[19] and density[20]) is affected by surface curvature, the C factor then becomes $C = (1 + p2r/L)$, where p is the ratio between the number of molecules per unit surface within the spherical and the cylindrical part. Higher solute concentrations within the less dense caps could be another source in underestimating the local order.

The radial intercalation of Orange Red can be described by relation 6b, obviously corrected by the foregoing C shape factor. In order to eliminate the assumption of the perfect guest–host alignment, it may be more convenient to have an expression which also displays the amount of preferred orientation of its z axis to the aggregate b axis by a S_m order parameter. This can be directly obtained from the general eq 5 by assuming the orientational degeneracy $S'_{xx} = S'_{yy} = -{}^1/_2S'_{zz}$ which is a very logical assumption for a nearly rod-like molecule as for instance Orange Red. Thus, by labeling $S'_{zz} = S_m$

$$(LD_r)_B = 3S_aS_m[-\tfrac{1}{2}(1 - \cos^2 \vartheta_{j,z}) + \cos^2 \vartheta_{jz}]$$

and then

$$(LD_r)_B = \tfrac{3}{2}S_aS_m(3\cos^2 \vartheta_{j,z} - 1) \quad (7)$$

$$(LD_r)_B^{cor} = \tfrac{3}{2}S_aS_m(3\cos^2 \vartheta_{j,z} - 1)/C \quad (7')$$

The $(S_{zz})_{max}$ of Table II may be considered to be the product of the S_m and S_a limiting values for perfect alignments which take the values of ($-{}^1/_2$, 1) for N_{C^+}, ($-{}^1/_2$, $-{}^1/_2$) for N_{C^-}, (1, 1) for N_{D^+}, and (1, $-{}^1/_2$) for N_{D^-} cases.

Shape-Correction Factor for Disk-like Micelles. In this case we must take into account a rim, with a half-torus shape, around the disk bilayer. The correction factor obtained for this case is

$$C' = [1 + (\pi h/2R)(1 + h/\pi R)]/(1 + \pi h/8R)$$

where h/R is the ratio between the thickness and the radius of the disk.[21] The values of this ratio reported in Table II had only been experimentally estimated for the N_D phases of mixtures 2 and 3.[8a] It is practically the same in both cases, and this encourages the transfer of its value also to the other disk-like micelles used throughout this investigation.

Corrected Order Parameters: $(S_{zz}^{exp})_{cor}$

The C and C' values were then computed by using the experimental estimates[8a] of r/L, or h/R (Table II). The correction factors were then multiplied by the (S_{zz}^{exp})'s to get the corrected $(S_{zz}^{exp})_{cor}$ values (Table II). The ratio $(S_{zz})_{max}/(S_{zz}^{exp})_{cor}$ is also reported in Table II in order to make a direct comparison between the two sets of values.

These (S_{zz}^{exp}) data for mixtures 2 and 3 are 44% of the theoretical maximum values $(S_{zz})_{max}$, in N_{C^+} media. This percentage is basically confirmed by mixture 1 if its r/L is assumed to be in the range of that found for the N_{C^+} phases of mixtures 2 or 3.

If we extend this guess to the N_{C^-} phase of mixture 4, its $(S_{zz}^{exp})_{cor}$ becomes much closer (88%) to the corresponding $(S_{zz})_{max}$ than the previous N_{C^+} phase values. The above-mentioned wall-anchorage effect may have significantly contributed to so high a value, although variations in the aggregate dimensions may be also be the cause. All the local order parameters exhibited by Orange Red, also within N_D micelles, are surprisingly high. Both N_{D^+} and N_{D^-} data of $(S_{zz}^{exp})_{cor}$ are in fact about 50% of the theoretical maximum ones.

The guest local ordering seems to be very poorly affected by changes in the micelle shape (see N_{C^+} and N_{D^-} phases of mixtures 2 and 3 in Table II).

Conclusions

The local ordering of Orange Red is very high within both disk-like and cylindrical micelles. The ability of lyotropic micelles

(17) Norden, B. *J. Chem. Phys.* **1980**, *72*, 5032–5038.

(18) Zasadzinski, J. A. N.; Sammon, M. J.; Kusma, M. R. AT&T Bell Laboratories Murray Hill N.J., private communication.

(19) (a) Hendrikx, Y.; Charvolin, J.; Rawiso, M. *J. Colloid Interface Sci.* **1984**, *100*, 597–600. (b) Alperine, S.; Hendrikx, Y.; Charvolin, J. *J. Phys. Lett.* **1985**, *46*, L27-31.

(20) Nakamura, T.; Kira, A.; Imamura, M. *J. Phys. Chem.* **1984**, *88*, 3435–3441.

(21) The components of the transition dipole moment μ of a molecule intercalated at the surface point P (Figure 2a) were obtained within the laboratory frame. They were transferred from the local (a_0, b_0, c_0) frame by using the usual formulas for transformation from one system of coordinates to another. The squares of the components of μ along the $\parallel$ and $\perp$ polarization directions ($\mu_\parallel^2$ and $\mu_\perp^2$), provide $E_\parallel$ and $E_\perp$. These $\mu_\parallel^2$ and $\mu_\perp^2$ expressions are then integrated over the rim for α from $-\pi/2$ to $+\pi/2$ (Figure 2a). In this integration the angle $d\alpha$ identifies ribbons which are $[h/2d\alpha]$ large and $[2\pi(R + h/2\cos\alpha)]$ long. The $E_\parallel$ and $E_\perp$ so obtained are inserted in formula 1, thus providing expression 7′ with the C' correction factor.

to force this guest molecule to assume an orientational distribution which is locally very anisotropic is certainly rather surprising if one takes into account the emphasis so far put on the inner disorder of the micellar aggregate.[2,3]

The intercalation of Orange Red within the host aggregates, perpendicular to their surfaces, is expected to be strongly stabilized by its highly anisotropic molecular shape and also by its ability to grasp at the polar micelle surface through its terminal dimethylamino group.[1]

In search for orientational effects in micellar catalysis[4] and in the hope that the control of stereochemistry by micelles will be more efficient in the future, the use of the LD technique may drive a true molecular-engineering approach to the reactivity and photochemistry in micellar aggregates.

It is of significance for photochemical applications of photoselection processes within micellar hosts that the *macroscopic linear anisotropy is highest within* N_{D^+} *micelles*. This provides the way in oriented lyotropic media to make the best use of the intrinsic anisotropy of the photochemical processes.[4]

Acknowledgment. This research was supported by CNR and MPI grants.

Registry No. KL, 10124-65-9; KHxOB, 108836-72-2; KHpOB, 96339-97-8; SdS, 142-87-0; dOH, 112-30-1; Orange Red, 2491-74-9.

Extending Surface-Enhanced Raman Spectroscopy to Transition-Metal Surfaces: Carbon Monoxide Adsorption and Electrooxidation on Platinum- and Palladium-Coated Gold Electrodes

Lam-Wing H. Leung and Michael J. Weaver*

Contribution from the Department of Chemistry, Purdue University, West Lafayette, Indiana 47907. *Received February 19, 1987*

Abstract: Thin (ca. one to three monolayers) films of platinum and palladium electrodeposited on electrochemically roughened gold are observed to yield surface-enhanced Raman (SER) spectra for adsorbed carbon monoxide. The major vibrational band(s) on these surfaces are diagnosed from their frequencies as arising from C–O stretching vibrations, ν_{CO}, for CO bound to the transition-metal overlayers rather than to residual gold sites. The observed SER ν_{CO} frequencies are closely similar to (within ca. 10 cm^{-1} of) those obtained for these systems from potential-difference infrared (PDIR) spectra. The major SERS and PDIR ν_{CO} features for the platinum and palladium surfaces appear at 2060–2090 and 1965–1985 cm^{-1}, respectively, consistent with the presence of "terminal" and "bridging" CO on these two electrodes. The infrared as well as electrochemical properties of these systems are closely similar to those for the corresponding polycrystalline "bulk" electrodes. A difference between the SER- and IR-active adsorbed CO, however, is that the former undergoes electrooxidation on both surfaces at 0.2–0.3 V higher overpotentials than the latter form. Examination of the potential-dependent SERS bands for metal oxide vibrations, ν_{PtO}, on the platinum surface shows that the electrooxidation potential for the SERS-active adsorbed CO coincides with that for the appearance of the ν_{PtO} band. Some broader implications to the utilization of SERS for examining transition-metal surfaces are pointed out.

Surface-enhanced Raman scattering (SERS) is now well established as a means of obtaining detailed information for a wide variety of adsorbates, especially in electrochemical environments.[1] However, despite the significant number of metals that have been predicted and/or demonstrated to yield the SERS effect, in practice this technique has been limited almost entirely to silver, gold, and copper surfaces.[1] While these metals, especially gold, are of considerable electrochemical significance, it is clearly of importance to develop means of extending the applicability of SERS to other surfaces.

One possible approach involves coating SERS-active metals with thin overlayers so that the chemical properties of the modified surface reflect primarily that of the overlayer material, yet maintaining SERS activity for species adsorbed on the overlayer by keeping them in suitably close proximity to the underlying substrate. We have recently demonstrated that underpotential deposited (upd) monolayers of mercury, thallium, and lead on electrochemically roughened gold electrodes yield surfaces displaying strong SERS activity for several adsorbates that are bound to the overlayer metal.[2] This behavior is comparable to that observed for adsorbates at upd monolayers of silver and copper on gold.[3] Gold provides an especially suitable substrate for this purpose from several standpoints. These include the availability of an electrochemical roughening procedure that yields especially stable as well as intense SERS,[4] the wide potential ranges that are amenable to study using gold, and the high stability of upd and other metallic deposits on this metal.

Given the importance of transition metals in surface chemistry, it is clearly of interest to ascertain if this approach can be utilized to examine SERS at surfaces formed by overlayers of such materials on gold. The electrodeposition of very thin transition-metal layers on noble metal substrates, including gold, has been the subject of a number of investigations, focusing on the electrosorptive and electrocatalytic properties of the resulting overlayer surfaces.[5] Overall, these studies show that the electrochemical properties of the metal overlayers mimic those for bulk electrodes of the deposited metal, even for film thicknesses down to one to two equivalent monolayers.[5]

(1) Recent reviews include: (a) Chang, R. K.; Laube, B. L. *CRC Crit. Rev. Solid State Mater. Sci.* **1984**, *12*, 1. (b) Moskovits, M. *Rev. Mod. Phys.* **1985**, *57*, 783. (c) Weitz, D. A.; Moskovits, M.; Creighton, J. A. In *Chemistry and Structure at Interfaces — New Laser and Optical Techniques*; Hall, R. B., Ellis, A. B., Eds.; VCH Publishers: Deerfield Beach, FL, 1986; p 197.

(2) Leung, L.-W. H.; Weaver, M. J. *J. Electroanal. Chem.* **1987**, *217*, 367.

(3) Leung, L.-W. H.; Gosztola, D.; Weaver, M. J. *Langmuir* **1987**, *3*, 45.

(4) (a) Gao, P.; Patterson, M. L.; Tadayyoni, M. A.; Weaver, M. J. *Langmuir* **1985**, *1*, 173. (b) Gao, P.; Gosztola, D.; Leung, L.-W. H.; Weaver, M. J. *J. Electroanal. Chem.*, in press.

(5) (a) Rand, D. A. J.; Woods, R. *J. Electroanal. Chem.* **1973**, *44*, 83. (b) Furuya, N.; Motoo, S. *Ibid.* **1978**, *88*, 151. (c) Motoo, S.; Shibata, M.; Watanabe, M. *Ibid.* **1983**, *110*, 103. (d) Lin-Cai, J.; Pletcher, D. *Ibid.* **1983**, *149*, 237.

0002-7863/87/1509-5113$01.50/0